Highlights:

- Acute ozone exposure only little effected physiological parameters of date palms.
- Anti-oxidants and turgor balance cooperatively mediate ozone tolerance.
- Local and systemic changes in metabolites contribute to the ozone tolerance.
- Root metabolism was impacted by ozone due to altered shoot - root interactions.

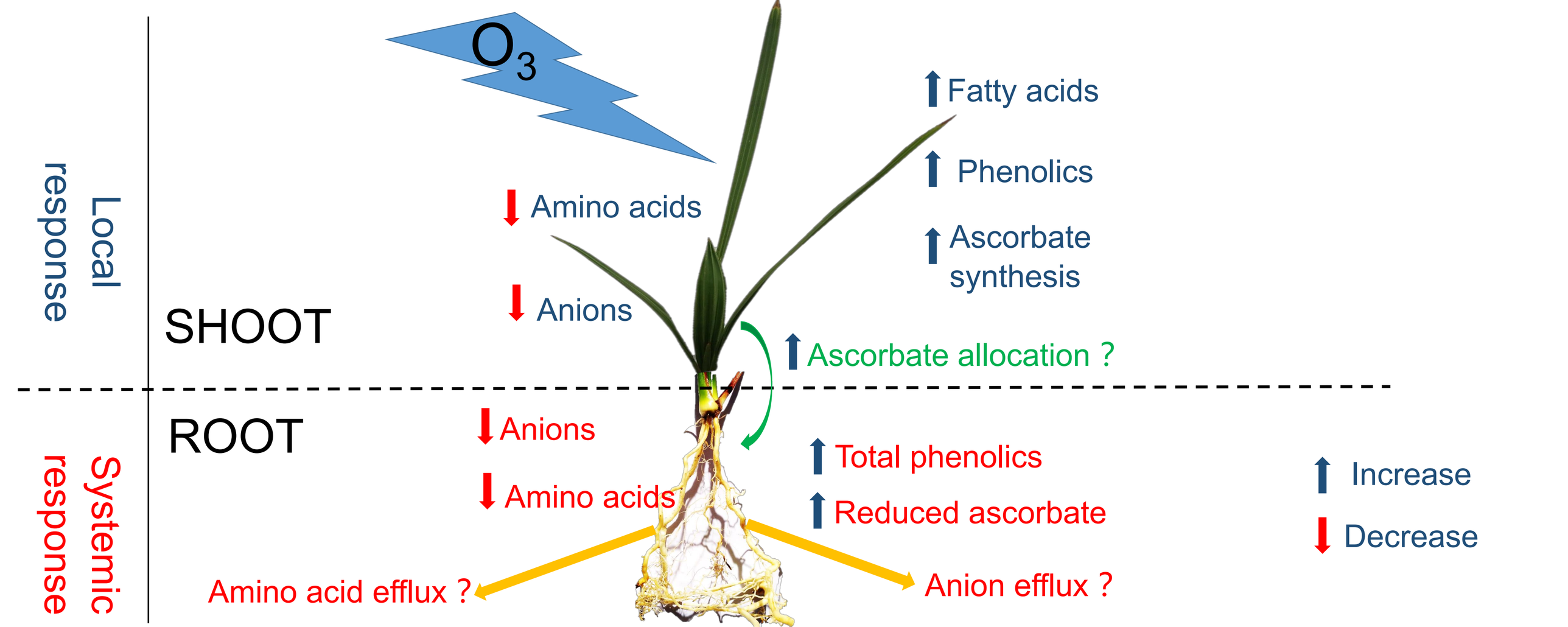
Local response
Systemic response
SHOOT
ROOT
O_3
Fatty acids
Phenolics
Ascorbate synthesis
Amino acids
Anions
Ascorbate allocation ?
Anions
Amino acids
Total phenolics
Reduced ascorbate
Amino acid efflux ?
Anion efflux ?
Increase
Decrease

Physiological responses of date palm (*Phoenix dactylifera*) seedlings to acute ozone exposure at high temperature

Baoguo Du[1, 2,*], Jürgen Kreuzwieser[2], Jana Barbro Winkler[3], Andrea Ghirardo[3], Jörg-Peter Schnitzler[3], Peter Ache[4], Saleh Alfarraj[6], Rainer Hedrich[4], Philip White[5], Heinz Rennenberg[2, 6]

[1] College of Life Science and Biotechnology, Mianyang Normal University; Mianxing Road West 166, 621000, Mianyang, China.

[2] Chair of Tree Physiology, Institute of Forest Sciences, Albert-Ludwigs-Universität Freiburg, Georges-Köhler-Allee 53, 79110 Freiburg, Germany.

[3] Helmholtz Zentrum München, Research Unit Environmental Simulation (EUS) at the Institute of Biochemical Plant Pathology (BIOP), Ingolstädter Landstraße 1, 85764 Neuherberg, Germany.

[4] Institute for Molecular Plant Physiology and Biophysics, Biocenter, University of Wuerzburg, 97082 Wuerzburg, Germany.

[5] The James Hutton Institute, Invergowrie, Dundee DD2 5DA, Scotland UK.

[6] King Saud University, PO Box 2455, Riyadh 11451, Saudi Arabia.

***Corresponding author: baoguo.du@ctp.uni-freiburg.de**

Abstract:

Vegetation in the Arabian Peninsula is facing high and steadily rising tropospheric ozone pollution. However, little is known about the impacts of elevated ozone on date palms, one of the most important indigenous economic species. To elucidate the physiological responses of date palm to peak levels of acute ozone exposure, seedlings were fumigated with 200 ppb ozone for 8 h. Net CO_2 assimilation rate, stomatal conduction, total carbon, its isotope signature and total sugar contents in leaves and roots were not significantly affected by the treatment and visible symptoms of foliar damage were not induced. Ozone exposure did not affect hydrogen peroxide and thiol contents but diminished the activities of glutathione reductase and dehydroascorbate reductase, stimulated the oxidation of ascorbate, and resulted in elevated total ascorbate contents. Total nitrogen, soluble protein and lignin contents remained unchanged upon ozone exposure, but the abundance of low molecular weight nitrogen (LMWN) compounds such as amino acids and nitrate as well as other anions were strongly diminished in leaves and roots. Other nitrogen pools did not benefit from the decline of LMWN, indicating reduced uptake and/or enhanced release of these compounds into the soil as a systemic response to aboveground ozone exposure. Several phenolic compounds, concurrent with fatty acids and stearyl alcohol, accumulated in leaves, but declined in roots, whereas total phenol contents significantly increased in the roots. Together these results indicate that local and systemic changes in both, primary and secondary metabolism contribute to the high tolerance of date palms to short-term acute ozone exposure.

Key words: sugars, reactive oxygen species, glutathione, ascorbate, nitrate, nitrogen partitioning, anti-oxidative system, secondary metabolites.

Capsule:

Date palms can grow and develop in an environment with high acute atmospheric ozone levels due to its tolerance to this air pollutant mediated by adaptations of both, primary and secondary metabolisms, as well as whole plant shoot-root interactions.

1. Introduction

Ozone (O_3) is not only an important greenhouse gas that contributes to climate change, but also a most damaging air pollutant to plants and ecosystems (Sandermann, 1996). Markedly rising tropospheric ozone concentrations have been documented both, in the industrialized parts of the world and in developing countries, at a rate of 1-5 ppb per decade; in the northern hemisphere, ground-level ozone concentrations doubled since 1950 (Cooper et al., 2014; Hartmann et al., 2013). The mean global tropospheric ozone levels are projected to further increase up to 80 ppb by 2100, with uncertain consequences for global forests (Moura et al., 2018; Paoletti et al., 2014).

Numerous deleterious physiological effects of ozone on plants have been observed, e.g., visible leaf injury, altered primary and secondary metabolisms, impaired hydraulic status, reductions in photosynthesis, and accelerated leaf senescence ((Dizengremel, 2001; Fares et al., 2013; Wittig et al., 2007). Thus, elevated levels of ozone will reduce the productivity and performances of economically important plants in both, agricultural and forest systems (Basahi et al., 2016).

Ozone is formed in the troposphere through a series of complex photochemical reactions from its precursors nitrogen oxides (NO_x), carbon monoxide (CO), methane (CH_4), and volatile organic compounds (VOCs) in the presence of sunlight. Since high temperature favors the production of ozone, the Middle East and particularly the Arabian Gulf region with high temperature, intense solar radiation, and clear sky, provide highly favorable conditions for ozone formation in summer (Radaideh, 2016; Smoydzin et al., 2012). Elevated ozone precursor emissions as well as increased levels of ozone have been documented over the entire Middle East (Smoydzin et al., 2012, and references therein), also as a consequence of accelerated urban development and growing industrialization (Radaideh, 2016). In addition to the significant ozone production from local pollution, there is also evidence that long distance transport of ozone precursors contributes to the

high level of ozone in the Middle East (Lelieveld et al., 2009). Air pollution and VOC emissions stimulate photo-oxidative processes in the troposphere of Western Europe and cause long distance transport of air pollutants generated in Western Europe to the Arabian Peninsula as well ozone production during this long-distance transport (Lelieveld et al., 2009; Reid et al., 2008). Consequently, vegetation on the Arabian Peninsula is subjected to high tropospheric ozone pollution from both regional and distant sources (Basahi et al., 2016). However, consequences of ozone pollution for growth and development of the vegetation on the Arabian Peninsula are largely unknown.

At the Arabian Peninsula, ozone pollution is of high significance for the date palm (*Phoenix dactylifera* L.), which is one of the most important indigenous food sources. From 1990 to 2011, total number and total area of date palm trees in Saudi Arabia have increased from 13 million to 25 million trees, and from 55,000 ha to 170,000 ha, respectively (Al-Redhaiman, 2014). Currently, almost one-third of the cultivated land of Saudi Arabia is planted with date palms, and the Kingdom is ranked as the second largest date producer in the world next to Egypt (Aleid et al., 2015). Therefore, there is a high interest to explore the physiological responses of date palms to ozone exposure.

The present study was aimed to characterize the physiological consequences of short-term exposure of young date palms to high but realistic ozone gas mixing ratios. Young date palms were chosen because they are assumed to be ozone sensitive as previously observed for other juvenile tree species (Nunn et al., 2005). It was hypothesized that ozone exposure 1) mediates a decline in stomatal conductance and photosynthesis; 2) leads to an accumulation of reactive oxygen species not prevented by the anti-oxidative system; and 3) results in changes of primary and secondary metabolic pathways.

2. Material and methods

2.1. Plant material and growth conditions

Seedlings of *Phoenix dactylifera*, *cv* Nabut Saif were purchased from a commercial nursery (Date Palm Developments Ltd., Sommerset, U.K.). They were directly planted in 5 L pots filled with 70% quartz gravel (3-5 mm diameter, Quarzwerke GmbH, Frechen, Germany) and covered by 3-5 cm soil substrate (Floragard Vertriebs-GmbH, Oldenburg, Germany). Seedlings were grown in walk-in phytotrons (area: 9.5 m^2), each containing four plexiglas subchambers (volume: 0.9 m^3 each) (Vanzo et al., 2015), at the Research Unit Environmental Simulation (EUS), Helmholtz Zentrum München (Neuherberg, Germany) at ambient CO_2 from 6th June to 27th July 2016. The initial conditions were 30 ^oC (12/12 h, day/night), 50% relative humidity, and then changed to experimental conditions (12/12 h day/night regime: rh 5% / 30%, temperature 40/20 ^oC, soil temperature 15 ^oC) within 3 days. After 3 weeks of acclimation, ozone fumigation was conducted as previously described (Kozovits et al., 2005; Strohm et al., 1999). For this purpose, a subset of plants was fumigated in sub-chambers with 200 ppb ozone from 10:00 to 18:00, while plants grown in other sub-chambers without ozone fumigation served as controls. Leaf and root samples of 6 individual plants from both, ozone treatments and controls were harvested after 1 h, 2 h, 4 h and 8 h of fumigation, respectively (Fig. 1). Harvested plant material was immediately homogenized in liquid nitrogen and stored at -80 ^oC until analyses.

Leaf gas exchange was determined (Figs. 1 and S1) by a portable gas exchange measuring system (GFS 3000, Walz GmbH, Effeltrich, Germany). For this purpose, fully expanded date palm leaves were placed into the 8 cm^2 cuvette of the system at a flow rate of 700 µmol s^{-1}, 400 ppm CO_2 and absolute water vapor of 8000 ppm. Light intensities inside the cuvette were set to a photosynthetic photon flux density (PPFD) of 1000 µmol m^{-2} s^{-1}. The leaf temperature was kept at 40 ^oC during the measurements. Photosynthesis (A), stomatal conductance (G) and intercellular CO_2 concentrations

(Ci) were manually recorded after CO_2 assimilation had stabilized. Intrinsic instantaneous water use efficiency was calculated as the ratio of A/G.

2.2. Determination of anti-oxidants, glutathione reductase (GR) and dehydroascorbate reductase (DHAR) activities, and hydrogen peroxide

The thiol anti-oxidant glutathione (GSH) and its metabolic precursors cysteine and γ-glutamylcysteine, as well as ascorbate were determined in plant material as previously described by Schupp and Rennenberg (1988) as modified by Samuilov et al. (2016). *In vitro* GR and DHAR activities of leaf and root material were determined as described previously (Arab et al., 2016). Hydrogen peroxide (H_2O_2) contents of leaf and root samples were determined as described by Velikova et al. (2000) (see Supplementary Text).

2.3. Determination of total sugar, soluble protein, lignin contents and phenolic compounds

To determine soluble sugar contents, 50 mg powdered frozen leaf and root samples were extracted with 1.5 mL of milliQ water at 95 °C for 5 min. After centrifugation, 200 µL of 10 times diluted supernatants were mixed with 1 mL anthrone reagent (50 mg anthrone and 1 g thiourea in 100 mL 70% H_2SO_4). The reaction solutions were boiled for 15 min and the absorbance measured at 578 nm (Carroll et al., 1956) after cooling down. Sucrose at 2 mmol was used as a standard.

Total soluble protein was quantified as previously described in Du et al. (2014). Lignin was extracted and determined as described by Moreira-Vilar et al. (2014) with some minor changes (see Supplementary Text).

147 Total phenolic compounds in plant samples were extracted with 50% acetone (Xu and Chang,
148 2007) and quantified by the Folin-Denis method using gallic acid as standard (see Supplementary
149 Text).
150
151 *2.4. Determination of ions and elements*
152
153 The anions nitrate (NO_3^-), phosphate (PO_4^{3-}) and sulphate (SO_4^{2-}) were determined in aqueous
154 extracts from homogenized frozen material by automated anion chromatography as described
155 previously (Peuke and Rennenberg, 2004). Element concentrations were determined following acid
156 digestion using Inductively Coupled Plasma Mass Spectrometry (ICP-MS) as described by White et
157 al. (2012) (see Supplementary Text).
158
159 *2.5. Extraction and determination of water soluble metabolites*
160 Relative abundances of water soluble low-molecular-weight metabolites in leaves and roots were
161 analyzed by Gas chromatography-mass spectrometry (GC-MS). For this purpose, metabolites were
162 extracted, derivatized and separated by a method modified from Kreuzwieser et al. (2009) (see
163 Supplementary Text). Identification of compounds was based on matching with the Golm
164 Metabolome Database (Hummel et al., 2010), compounds with match factor < 60 were excluded.
165
166 *2.6. Determination of leaf and roots hydration*
167

168 Leaf and root hydration (g H_2O g^{-1} dw) was determined as (fw - dw) dw^{-1}, where fw is the fresh
169 mass, and dw is the dry mass after drying the samples in an oven at 60 °C for 48 h (Arab et al., 2016)
170 .
171
172 *2.7. Statistical analysis*
173
174 Statistical analysis was performed with four (gas exchange data) or six (biochemical parameters)
175 biological replicates for both controls and ozone exposure across different fumigation time.
176 Significant differences ($P < 0.05$) between ozone exposed plants and controls within the same time
177 and tissues, and differences between leaves and roots of either ozone exposed plants or controls after
178 8 h fumigation, were examined by t tests. Data were first tested by the Shapiro-Wilk tests for normal
179 distribution. If required, raw data were transformed to denary logarithms to satisfy the assumptions
180 of normality. When data transformation did not fulfill the requirements of normal distribution, the
181 Mann-Whitney Rank Sum Test was employed. As little diurnal variations were observed (data not
182 shown), gas exchange parameters measured after 1 h, 4 h and 7 h and foliar contents of thiols,
183 ascorbate, anions and ions measured after 1 h, 2 h, 4 h and 8 h were pooled separately for controls
184 and ozone exposure.
185 SigmaPlot 11.0 (Systat Software GmbH, Erkrath, Germany) was employed for statistical
186 analysis and generation of figures. Fold change of different parameters was calculated as $\log_2$ (ozone
187 exposure / control); color gradients for different values were obtained by the functions of Conditional
188 formatting in Microsoft Excel 2013 (Microsoft Corporation, Redmond, WA, USA).
189

3. Results

3.1. Short-term exposure to acute ozone did not damage the leaves and did not affect their CO_2/H_2O gas exchange

Visible symptoms of injury such as de-coloration, dehydration or necrosis, typical for acute ozone exposure, were not observed on the leaf surfaces as well the on leafstalks of date palm seedlings. Also leaf gas exchange parameters were not impacted by the 8 h ozone exposure (Fig. S1). On average, net CO_2 assimilation rates slightly declined from 4.99 µmol m^{-2} s^{-1} of control plants to 3.92 µmol m^{-2} s^{-1} of ozone exposed plants ($P = 0.311$) (Fig. S1 A), and stomata conductance varied between 57.18 mmol m^{-2} s^{-1} and 39.29 mmol m^{-2} s^{-1}, respectively (Fig. S1 B). However, these changes were not statistically significant ($P > 0.05$). Also total carbon (C) content, instantaneous intrinsic water use efficiency (iWUE, Fig. S1 C) and the ratio between intracellular and ambient CO_2 concentration (Ci/Ca, Fig. S1 D), as well as leaf and root hydration and $\delta^{13}C$ signature (Table S1) were not affected by the ozone treatment. Further, total soluble sugar contents and sugar transport were not significantly impacted by 8 h ozone exposure (Fig. 2 A), consistent with largely conserved abundances of individual sugars, sugar alcohols and sugar acids (Fig. 3). After 8 h ozone fumigation, still fumaric acid and ribonic acid significantly accumulated in the leaves (Fig. 3).

3.2. Acute ozone exposure affected the anti-oxidative system at the level of ascorbate and anti-oxidative enzymes in leaves, but not in roots

The short-term ozone treatment did not affect hydrogen peroxide contents in leaves and roots (Table S1). Consistent with this observation, total and oxidized glutathione contents as well as the

214 contents of its metabolic precursors cysteine and γ-glutamylcysteine were not significantly impacted
215 by the ozone exposure, both in leaves and in roots (Fig. 4 A-D). However, total ascorbate contents
216 were generally enhanced in ozone exposed plants, particularly after 8 h fumigation (Fig. 4 E). In
217 addition, reduced ascorbate contents significantly increased in roots after 8 h ozone fumigation (Fig.
218 4 F). Dehydroascorbate contents in leaves were significantly increased after 1 h ozone fumigation
219 and, consequently, the ratio between reduced and oxidised ascorbate declined (Fig. 4 G and H).
220 Compared to not fumigated control plants, glutathione reductase (GR) activity in leaves
221 significantly ($P = 0.014$) decreased already after 1 h of ozone fumigation, (Fig. 5 A). Also,
222 dehydroascorbate reductase (DHAR) activity in leaves declined significantly after 2 h ($P = 0.033$)
223 and 8 h ($P = 0.045$) of ozone treatments (Fig. 5 B). No significant impact of ozone treatment on GR
224 and DHAR activities were found in the roots after 8 h fumigation (Fig. 5).
225
226 *3.3. Ozone exposure strongly diminished low molecular weight nitrogen metabolite and anion*
227 *contents*
228
229 Although contents of total nitrogen (N), soluble protein and lignin as well as $\delta^{15}N$ signatures in
230 leaves and roots were not significantly changed by ozone exposure, low molecular weight nitrogen
231 compounds (LMWN) declined in ozone fumigated plants; particularly the amino acid proline
232 significantly decreased in the leaves (Fig. 3). Slight increases in leaves, but decreases in roots, were
233 observed for the amino acids glutamic acid, γ-aminobutyric acid (GABA), uracil, ethanolamine and
234 leucine (Fig. 3).
235 Ozone treatment immediately reduced the contents of the anions NO_3^-, PO_4^{3-} and SO_4^{2-} in leaves
236 and roots and this decrease was maintained for the entire time of fumigation. It was particularly

pronounced for NO_3^- in both, leaves and roots. In addition, significant effects of the ozone treatment were observed for Cl and Mn contents. Compared to control plants, Cl contents in leaves declined already after 1 h fumigation, but increased significantly in roots after 8 h fumigation. Mn contents in leaves decreased significantly as an average of the 8 h ozone treatment (Table S2).

3.4. Ozone exposure modified the contents of phenolic compounds and fatty acids in leaves and roots

After 8 h ozone exposure, abundances of catechin, trans-4-caffeoylquinic acid and particularly 4-hydroxy-benzoic acid were up-regulated in both leaves and roots, while abundances of taxifolin, guaiacylglycerol, trans-sinapyl alcohol and cis-sinapic acid strongly increased in leaves, but decreased in roots (Fig. 3). No significant effects of ozone exposure on total phenolic compounds were observed in leaves, but a significantly accumulation in roots, after 8 h fumigation (Fig. 2 C). Ozone fumigation also resulted in enhanced foliar abundance of fatty acids and stearyl alcohol, particularly palmitic acid and stearic acid, but reduced the abundance of these metabolites in roots (Fig. 3).

3.5. Carbon and total sugar partitioning between leaves and roots and its responses to short-term acute ozone exposure

Total C and total soluble sugar contents did not significantly differ between leaves and roots (Fig. 2 A, Table S1), but individual sugars, i.e., the monosaccharide glucose and galactose, the disaccharides D-cellobiose, D-α, α'-trehalose, sophorose and gentiobiose were more abundant in leaves, whereas fructose, lyxose, sucrose, and the trisaccharides raffinose and 6-kestose levels were

higher in roots. Sugar acids except galactonic acid, sugar alcohols, and fatty alcohols were also more abundant in leaves than in roots. Contents of organic acids involved in the tricarboxylic acid (TCA) cycle as well as glycerol-3-P, mannose-6-P and shikimic acid were higher in roots than leaves (Fig. 3). Leaves had a more negative $\delta^{13}C$ signature and lower C/N ratio, as well as lower water content compared to the roots (Table S1). Levels of H_2O_2 and ascorbate were higher in leaves than roots, while no clear differences in thiol contents between leaves and roots were observed, except for cysteine which was higher in roots than in leaves (Fig. 4, Table S1). In contrast to the unsaturated fatty acid oleic acid, saturated fatty acids were more enriched in roots. (Fig. 3). Leaves had significantly ($P < 0.001$) higher contents of total N, soluble protein, but lower lignin contents compared to roots (Fig. 2, Table S1). Individual amino acids were more abundant in roots than in leaves except for proline (Fig. 3). Contents of PO_4^{3-}, total P, Ca and Mn were significantly higher in leaves than roots, while NO_3^- and Na were more abundant in roots (Table S2). Total phenolic compounds were much higher in leaves than in roots ($P < 0.001$), especially for catechin and guaiacylglycerol (Figs. 4 C and 5),

These partitioning patterns between leaves and roots were largely not affected by ozone fumigation except for ribonic acid, trans-sinapyl alcohol, cis-sinapic acid, which were accumulated in favor of leaves, whereas carbodiimine was accumulated in favor of roots (Fig. 3). Ozone exposure aggravated the differences between leaves and roots in the abundance of sucrose, D- α, α'-trehalose, malic acid, ribonic acid, the amino acids of aspartate family (i.e., aspartic acid, asparagine and threonine), serine, glycine, as well as tryptophan and pyroglutamic acid (Fig. 3), and the DHA contents (Fig. 4 G).

4. Discussion

4.1. Ozone effects on leaves

Most broad-leaved tree species use stomatal control as a 'first line of defense' to restrict the ozone flux into leaves (Wittig et al., 2007; Vainonen and Kangasjärvi, 2015). In the present study with date palm seedlings, neither significant effects on net CO_2 assimilation and stomatal conductance, nor visible leaf injury, i.e., bleaching, flecking and stippling, commonly reported in broad-leaved plants (Iriti and Faoro, 2009), were observed upon short-term exposure to acute ozone levels. Thus, the first hypothesis of this study (see: Introduction) has to be rejected. The obviously high tolerance of net CO_2 assimilation and stomatal conductance in *P. dactylifer*a to acute ozone exposure is shared with other tree species that developed traits of water saving strategies, such as *Picea*, *Pinus* or *Quercus* species (Fares et al., 2013; Wittig et al., 2007). In addition, the present results are consistent with a previous study on date palm seedlings, showing that neither heat nor moderate water-shortage had a significant effect on stomatal conductance (Arab et al., 2016).

Ozone that has entered the apoplastic space of the leaf is immediately degraded to secondary reactive oxygen species (ROS), including hydrogen peroxide (H_2O_2), superoxide and hydroxyl radicals (Vainonen and Kangasjärvi, 2015). However, in the present experiments foliar H_2O_2 levels of date palm leaves were kept constant during ozone exposure, as also observed in a heat and moderate drought treatment (Arab et al., 2016). Therefore, also hypothesis 2 of the present study (see: Introduction) has to be rejected. Since ROS levels in plant tissues constitute a balance between production and scavenging, unchanged foliar H_2O_2 levels at enhanced production should be a consequence of increased scavenging (Ahmed et al., 2015; Conklin and Barth, 2004). The conversion of ozone with ascorbate in the apoplastic space is considered the initial reaction of ozone scavenging

306 and secondary ROS production that is thought to determine ozone sensitivity of the leaves (Conklin
307 and Barth, 2004). Thus, elevating the level of apoplastic ascorbate and/or its enhanced recycling in
308 the Foyer-Halliwell-Asada cycle is supposed to be a more efficient protection against oxidative
309 damage than reducing stomatal conductance that will impair photosynthetic CO_2 fixation (Chen and
310 Gallie, 2005). In the present experiments, total ascorbate and DHA levels increased upon ozone
311 exposure, whereas reduced ascorbate was kept constant (Fig. 4 E-G), indicating enhanced ROS
312 scavenging as also observed in *Sedum album* leaves (Castillo and Greppin, 1988). On the other hand,
313 diminished *in vitro* GR and DHAR activities at enhanced DHA levels suggest reduced ascorbate
314 regeneration capacity by the Foyer-Halliwell-Asada cycle in date palm leaves upon ozone exposure.
315 At the same time, increased threonic acid and threonic acid-1,4-lactone levels (Fig. 3) indicate
316 enhanced DHA turnover (Simpson and Ortwerth, 2000) and increased levels of galactose, gluconic
317 acid-1,4-lactone, myo-inositol and galactonic acid (Fig. 3) imply enhanced ascorbate synthesis
318 (Dumont et al., 2014; Linster and Clarke, 2008). Thus, extention of ascorbate recycling in the Foyer-
319 Halliwell-Asada cycle by enhanced ascorbate synthesis and turnover may have contributed to the
320 high tolerance to acute ozone levels of date palm leaves. This conclusion is consistent with the
321 assumption of Dizengremel et al. (2008) that elevated apoplastic ascorbate levels alone may not be
322 sufficient to explain ozone tolerance. To test this conclusion, metabolite flux analyses should be
323 included in future ozone exposure experiments.

324 Despite enhanced ROS scavenging in the apoplastic space, primary metabolic pathways are
325 supposed to be affected by acute ozone exposure, in particular glycolysis, the TCA cycle and the
326 pentose phosphate pathway, to meet the enhanced requirement for NADPH in ozone defense
327 reactions (Dizengremel, 2001). This view is supported by the present results showing enhanced levels
328 of intermediates of these pathways (Fig. 3) and, therefore, is in favor of hypothesis 3 of this study

329 (see: Introduction). However, foliar amino acid contents of date palm seedling were diminished by
330 acute ozone exposure (Fig. 3), as previously observed in experiments with other species (Dumont et
331 al., 2014; Kainulainen et al., 1993). In date palm leaves, this decrease was not sufficient to cause
332 significantly reduced total N contents and cannot be attributed to an enhanced use of N in protein or
333 lignin biosynthesis (Fig. 2, Table S1). It may rather be an indication of reduced N assimilation as a
334 consequence of reduced foliar availability of NO_3^- (Table S2). In contrast to other abiotic stresses
335 (i.e., salt, drought, cold, heat, and abscisic acid) that mediated elevated foliar proline levels in date
336 palm seedlings (Yaish, 2015), proline was significantly decreased in ozone exposed date palm leaves,
337 thereby contributing to a reduced foliar LMWN content (Fig. 3). Apparently, foliar proline contents
338 did not contribute to the high tolerance of date palm leaves to acute ozone exposure.

339 In addition to NO_3^-, also other anions were strongly diminished in ozone exposed date palm leaves,
340 whereas cation contents were largely unaffected. Such a decline in anion contents has so far not been
341 reported, but may be required to balance the consumption of protons in ozone detoxification reactions
342 and, thus, may constitute means to enhance ozone tolerance (Vainonen and Kangasjärvi, 2015). In
343 this context, Cl^- may be of particular significance, because most of its functions are related to
344 electrical charge and turgor balance (Hänsch and Mendel, 2009). In addition, enhanced amounts of
345 NO_3^- have been reported to increase the sensitivity of soybeans plants to ozone (Smith et al., 1990).
346 Therefore, also the present decline of foliar NO_3^- contents may have contributed to the high tolerance
347 of date palm seedlings to elevated ozone.

348 Many studies have suggested close similarities between ozone- and pathogen-induced defense
349 responses in plants (Conklin and Barth, 2004; Iriti and Faoro, 2009). This is of particular significance
350 for the secondary metabolism that is not only involved in plant defense reactions against herbivores
351 and pathogens, but also in the response to a wide range of abiotic stresses (Ahmed et al., 2015; Witzell

and Martín, 2008). It has been hypothesized that any stress that suppresses growth more than photosynthesis, leads to an accumulation of secondary compounds, such as phenolics and isoprenoids, but also of fatty acids that serve as carbon sinks (Niinemets, 2015). Ozone induced accumulation of phenolic compounds including lignin have been reported in various tree species (Andersen, 2003; Dizengremel, 2001; Saleem et al., 2001; Strohm et al., 1999). Consistent with hypothesis 3 (see: Introduction), also in the present study with date palm seedlings, secondary metabolism responded strongly to acute ozone exposure. This is indicated by the accumulation of individual phenolic compounds and fatty acids (Fig. 3). However, total foliar phenolic and lignin contents remained unchanged (Fig. 2 C, D). Similar responses to elevated ozone were reported in leaves of European silver birch (*Betula pendula* Roth) with a preferential carbon allocation towards defensive phenolic compounds such as benzoic acid derivatives (Saleem et al., 2001). These metabolites are not only able to detoxify ROS (Ahmed et al., 2015; Witzell and Martín, 2008), but also to prevent ROS generation by metal chelation and, therefore, may even be more efficient anti-oxidants than ascorbate and α-tocopherol (Soobrattee et al., 2005).

The primary target of ozone damage to the leaves is the plasmalemma, since ozone is a potent oxidizing agent which reacts strongly with the double bond of unsaturated fatty acids. Therefore, ozone sensitivity is highly dependent on the composition and content of membrane fatty acids (Anttonen et al., 1995). In the present study, two saturated membrane fatty acids, i.e., palmitic acid and stearic acid, were highly abundant in ozone exposed leaves. Similar effects of ozone on palmitic acid and stearic acid were found in Aleppo pine (*Pinus halepensis* Mill.) needles (Anttonen et al., 1995). It can therefore be concluded that ozone mediated changes in the fatty acid composition of foliar membranes may also have contributed to the high tolerance of date palm leaves to acute ozone exposure.

375 *4.2. Ozone effects on roots and shoot-root interactions*

376

377 Because of its high reactivity, ozone cannot penetrate the soil and also cannot be subjected to long-
378 distance transport inside the plant. Therefore, responses of the root system to ozone exposure of the
379 leaves are systemic and cannot be attributed to direct ozone action. In the present study, such systemic
380 effects of ozone exposure were rare, but included a significant increase of reduced ascorbate in roots
381 by 24% (Fig. 4 F). Since ascorbate levels in the roots are thought to be determined by shoot-to-root
382 allocation rather than biosynthesis in the roots (Herschbach et al., 2009), this result indicates enhanced
383 phloem transport of ascorbate although stimulated ascorbate biosynthesis in the roots cannot be
384 excluded from the present experiments. This view is consistent with the observation that carbohydrate
385 allocation from the leaves to the roots is not impaired upon acute ozone exposure of date palm leaves,
386 as indicated by leaf and root carbohydrate contents (Fig. 2 A). Reduced export of carbohydrate from
387 source leaves has been reported upon ozone exposure for several plant species (Dizengremel, 2001;
388 Grantz and Farrar, 2000; Zheng et al., 2000), but was not observed in ozone resistant loblolly pine
389 (Spence et al., 1990) and wheat (Mortensen and Engvild, 1995). Apparently, also ozone insensitive
390 phloem transport may have contributed to the high tolerance of date palm seedlings to acute ozone
391 exposure. Therefore, it is not surprising that general partitioning profiles between shoots and roots
392 were independent of ozone exposure in date palm seedlings (Figs 4-7, Table S1 and S2). This
393 partitioning profiles included significantly higher amounts of total N, soluble protein, and phenolic
394 compounds in the leaves, but lower contents of lignin and most amino acids except for proline (Figs.
395 4 and 5, Table S1). Similarly, higher lignin contents, but lower amounts of total N and phenolic
396 compounds in roots than in leaves were reported in several agroforestry species (Vanlauwe et al.,
397 1996). This partitioning pattern was also observed for individual secondary metabolites, including
398 the phenolic compounds catechin and guaiacylglycerol, the unsaturated fatty acid oleic acid and fatty

399 alcohols (Fig. 3), as previously observed by Niazwali (2016). Still ozone exposure reversed the
400 partitioning differences between leaves and roots for individual metabolites, such as ribonic acid, cis-
401 sinapic acid, trans-sinapyl alcohol and myo-inositol, due to foliar accumulations of these compounds
402 (Fig. 3), as also reported for other tree species (Andersen, 2003; Dizengremel, 2001; Saleem et al.,
403 2001).

404 As observed for the leaves, anion contents of the roots declined upon ozone exposure of the leaves.
405 This systemic effect cannot be attributed to enhanced allocation to the leaves (Table S2). For nitrate
406 and sulfate also enhanced assimilation in the roots can be excluded, because protein, thiol, and lignin
407 contents of the roots were not affected and amino acid contents even declined upon acute ozone
408 exposure (Figs. 4-6). Therefore, the ozone mediated reduction in anion contents may be attributed to
409 reduced uptake and/or enhanced exudation into the rhizosphere. Inorganic anion exudation into the
410 rhizosphere may be necessary to regulate the pH in root cells by electrically counterbalancing the
411 efflux of protons, or/and to regulate whole plant inorganic anion acquisition under stressful conditions
412 (Kollist et al., 2011).

413 .

414 **5. Conclusions**
415

416
417 The present results show that date palm seedlings are highly resistant to acute ozone exposure and
418 that this high tolerance is a consequence of a whole set of fast acclimation reactions indicating local
419 and systemic responses. These reactions include strengthening of the anti-oxidative system, electrical
420 charge and turgor balance by reduced uptake and/or enhanced exudation on anions, as well as changes
421 in primary metabolites, phenolic compounds and fatty acids. It is suggested that the concerted action
422 of these processes provide an essential background for the successful growth and development of date
423 palms in an environment prone to high atmospheric ozone gas mixing ratios (Lelieveld et al., 2009).

Declarations of interest:

none.

Acknowledgement:

Financial support of this study by King Saud University, Riyadh, Saudi Arabia in the frame of the Distinguished Scientists Program is gratefully acknowledged. The authors thank Dr. Leila Arab for her help during harvest and gas exchange measurements.

References

Ahmed, I.M., Nadira, U.A., Bibi, N., Cao, F., He, X., Zhang, G., Wu, F., 2015. Secondary metabolism and antioxidants are involved in the tolerance to drought and salinity, separately and combined, in Tibetan wild barley. Environ. Exp. Bot. 111, 1–12.

Aleid, S.M., Al-Khayri, J.M., Al-Bahrany, A.M., 2015. Date palm status and perspective in Saudi Arabia, in: Date Palm Genetic Resources and Utilization. Springer, pp. 49–95.

Al-Redhaiman, K.N., 2014. Date Palm Cultivation in Saudi Arabia: Current Status and Future Prospects for Development [WWW Document]. 2014 ASHS Conf. Meet. Abstr. URL http://hortsci.ashspublications.org/content/49/9/suppl/DC1 (accessed 9.19.17).

Andersen, C.P., 2003. Source–sink balance and carbon allocation below ground in plants exposed to ozone. New Phytol. 157, 213–228.

Anttonen, S., Herranen, J., Peura, P., Kärenlampi, L., 1995. Fatty acids and ultrastructure of ozone-exposed Aleppo pine (*Pinus halepensis* Mill.) needles. Environ. Pollut. 87, 235–242.

Arab, L., Kreuzwieser, J., Kruse, J., Zimmer, I., Ache, P., Alfarraj, S., Al-Rasheid, K.A., Schnitzler, J.-P., Hedrich, R., Rennenberg, H., 2016. Acclimation to heat and drought—Lessons to learn from the date palm (*Phoenix dactylifera*). Environ. Exp. Bot. 125, 20–30.

Basahi, J.M., Ismail, I.M., Haiba, N.S., Hassan, I.A., Lorenzini, G., 2016. Assessing ambient ozone injury in olive (*Olea europaea* L.) plants by using the antioxidant ethylenediurea (EDU) in Saudi Arabia. Environ. Monit. Assess. 188, 371. https://doi.org/10.1007/s10661-016-5376-2.

Carroll, N.V., Longley, R.W., Roe, J.H., 1956. The determination of glycogen in liver and muscle by use of anthrone reagent. J. Biol. Chem. 220, 583–593.

453 Castillo, F.J., Greppin, H., 1988. Extracellular ascorbic acid and enzyme activities related to ascorbic
454 acid metabolism in *Sedum album* L. leaves after ozone exposure. Environ. Exp. Bot. 28, 231–
455 238.
456 Chen, Z., Gallie, D.R., 2005. Increasing tolerance to ozone by elevating foliar ascorbic acid confers
457 greater protection against ozone than increasing avoidance. Plant Physiol. 138, 1673–1689.
458 Conklin, P.L., Barth, C., 2004. Ascorbic acid, a familiar small molecule intertwined in the response
459 of plants to ozone, pathogens, and the onset of senescence. Plant Cell Environ. 27, 959–970.
460 Cooper, O.R., Parrish, D.D., Ziemke, J., Balashov, N.V., Cupeiro, M., Galbally, I.E., Gilge, S.,
461 Horowitz, L., Jensen, N.R., Lamarque, J.F., 2014. Global distribution and trends of
462 tropospheric ozone: An observation-based review. Elem Sci Anth 2.
463 https://doi.org/10.12952/journal.elementa.000029
464 Dizengremel, P., 2001. Effects of ozone on the carbon metabolism of forest trees. Plant Physiol.
465 Biochem. 39, 729–742.
466 Dizengremel, P., Le Thiec, D., Bagard, M., Jolivet, Y., 2008. Ozone risk assessment for plants: central
467 role of metabolism-dependent changes in reducing power. Environ. Pollut. 156, 11–15.
468 Du, B., Jansen, K., Junker, L.V., Eiblmeier, M., Kreuzwieser, J., Gessler, A., Ensminger, I.,
469 Rennenberg, H., 2014. Elevated temperature differently affects foliar nitrogen partitioning in
470 seedlings of diverse Douglas fir provenances. Tree Physiol. 34, 1090–1101.
471 Dumont, J., Keski-Saari, S., Keinänen, M., Cohen, D., Ningre, N., Kontunen-Soppela, S., Baldet P,
472 Gibon Y, Dizengremel P, Vaultier MN, Jolivet Y, Oksanen E, Le Thiec D. 2014. Ozone
473 affects ascorbate and glutathione biosynthesis as well as amino acid contents in three
474 Euramerican poplar genotypes. Tree Physio. 34, 253-266.

475 Fares, S., Vargas, R., Detto, M., Goldstein, A.H., Karlik, J., Paoletti, E., Vitale, M., 2013.
476 Tropospheric ozone reduces carbon assimilation in trees: estimates from analysis of
477 continuous flux measurements. Glob. Change Biol. 19, 2427–2443.
478 Grantz, D.A., Farrar, J.F., 2000. Ozone inhibits phloem loading from a transport pool: compartmental
479 efflux analysis in Pima cotton. Funct. Plant Biol. 27, 859–868.
480 Hänsch, R., Mendel, R.R., 2009. Physiological functions of mineral micronutrients (Cu, Zn, Mn, Fe,
481 Ni, Mo, B, Cl). Curr. Opin. Plant Biol. 12, 259–266.
482 Hartmann, D.L., Tank, A.M.K., Rusticucci, M., Alexander, L.V., Brönnimann, S., Charabi, Y.A.R.,
483 Dentener, F.J., Dlugokencky, E.J., Easterling, D.R., Kaplan, A., 2013. Observations:
484 atmosphere and surface, in: Climate Change 2013 the Physical Science Basis: Working Group
485 I Contribution to the Fifth Assessment Report of the Intergovernmental Panel on Climate
486 Change. Cambridge University Press, Cambridge, UK, pp. 159–254.
487 Herschbach, C., Scheerer, U., Rennenberg, H., 2009. Redox states of glutathione and ascorbate in
488 root tips of poplar (*Populus tremula* × *P. alba*) depend on phloem transport from the shoot to
489 the roots. J. Exp. Bot. 61, 1065–1074.
490 Hummel, J., Strehmel, N., Selbig, J., Walther, D., Kopka, J., 2010. Decision tree supported
491 substructure prediction of metabolites from GC-MS profiles, Metabolomics 6, 322-333.
492 Iriti, M., Faoro, F., 2009. Chemical diversity and defence metabolism: how plants cope with
493 pathogens and ozone pollution. Int. J. Mol. Sci. 10, 3371–3399.
494 Kainulainen, P., Holopainen, J.K., Hyttinen, H., Oksanen, J., 1993. Effect of ozone on the
495 biochemistry and aphid infestation of Scots pine. Phytochemistry 35, 39–42.
496 Kollist, H., Jossier, M., Laanemets, K., Thomine, S., 2011. Anion channels in plant cells. FEBS J.
497 278, 4277–4292.

Kozovits, A.R., Matyssek, R., Blaschke, H., Göttlein, A., Grams, T.E., 2005. Competition increasingly dominates the responsiveness of juvenile beech and spruce to elevated CO_2 and/or O_3 concentrations throughout two subsequent growing seasons. Glob. Change Biol. 11, 1387–1401.

Kreuzwieser, J., Hauberg, J., Howell, K.A., Carroll, A., Rennenberg, H., Millar, A.H., Whelan, J., 2009. Differential response of gray poplar leaves and roots underpins stress adaptation during hypoxia. Plant Physiol. 149, 461–473.

Lelieveld, J., Hoor, P., Jöckel, P., Pozzer, A., Hadjinicolaou, P., Cammas, J.-P., Beirle, S., 2009. Severe ozone air pollution in the Persian Gulf region. Atmospheric Chem. Phys. 9, 1393–1406.

Linster, C.L., Clarke, S.G., 2008. L-Ascorbate biosynthesis in higher plants: the role of VTC2. Trends Plant Sci. 13, 567–573.

Moreira-Vilar, F.C., de Cássia Siqueira-Soares, R., Finger-Teixeira, A., de Oliveira, D.M., Ferro, A.P., da Rocha, G.J., Maria de Lourdes, L.F., dos Santos, W.D., Ferrarese-Filho, O., 2014. The acetyl bromide method is faster, simpler and presents best recovery of lignin in different herbaceous tissues than klason and thioglycolic acid methods. PLoS One 9, e110000.

Mortensen, L., Engvild, K.C., 1995. Effects of ozone on ^{14}C translocation velocity and growth of spring wheat (*Triticum aestivum* L.) exposed in open-top chambers. Environ. Pollut. 87, 135–140.

Moura, B.B., Alves, E.S., Marabesi, M.A., de Souza, S.R., Schaub, M. and Vollenweider, P., 2018. Ozone affects leaf physiology and causes injury to foliage of native tree species from the tropical Atlantic Forest of southern Brazil. Sci. Total Environ. 610, 912-925.

Niazwali, S. A., 2016. Examining the growth and performance of the effect of UV-B radiation on United Arab Emirates Date Palm Tree (*Phoenix dactylifera*). Master thesis, United Arab Emirates University, Abu Dhabi, UAE.

Niinemets, Ü., 2015. Uncovering the hidden facets of drought stress: secondary metabolites make the difference. Tree Physiol. 36, 129–132.

Nunn, A.J., Kozovits, A.R., Reiter, I.M., Heerdt, C., Leuchner, M., Lütz, C., Liu, X., Lo, M., Winkler, J.B., Grams, T.E.E., 2005. Comparison of ozone uptake and sensitivity between a phytotron study with young beech and a field experiment with adult beech (*Fagus sylvatica*). Environ. Pollut. 137, 494–506.

Paoletti, E., De Marco, A., Beddows, D.C., Harrison, R.M., Manning, W.J., 2014. Ozone levels in European and USA cities are increasing more than at rural sites, while peak values are decreasing. Environ. Pollut. 192, 295–299.

Peuke, A.D., Rennenberg, H., 2004. Carbon, nitrogen, phosphorus, and sulphur concentration and partitioning in beech ecotypes (*Fagus sylvatica* L.): phosphorus most affected by drought. Trees 18, 639–648.

Polle, A., Chakrabarti, K., Schürmann, W., Renneberg, H., 1990. Composition and properties of hydrogen peroxide decomposing systems in extracellular and total extracts from needles of Norway spruce (*Picea abies* L., Karst.). Plant Physiol. 94, 312–319.

Radaideh, J.A., 2016. Industrial air pollution in Saudi Arabia and the influence of meteorlogical variables. Environ. Sci. Technol. 1, 334–345.

Reid, J.S., Piketh, S.J., Walker, A.L., Burger, R.P., Ross, K.E., Westphal, D.L., Bruintjes, R.T., Holben, B.N., Hsu, C., Jensen, T.L., 2008. An overview of UAE2 flight operations:

542 Observations of summertime atmospheric thermodynamic and aerosol profiles of the southern
543 Arabian Gulf. J. Geophys. Res. Atmospheres 113. https://doi.org/10.1029/2007JD009435
544 Saleem, A., Loponen, J., Pihlaja, K., Oksanen, E., 2001. Effects of long-term open-field ozone
545 exposure on leaf phenolics of European silver birch (*Betula pendula* Roth). J. Chem. Ecol. 27,
546 1049–1062.
547 Samuilov, S., Lang, F., Djukic, M., Djunisijevic-Bojovic, D., Rennenberg, H., 2016. Lead uptake
548 increases drought tolerance of wild type and transgenic poplar (*Populus tremula* x *P. alba*)
549 overexpressing gsh 1. Environ. Pollut. 216, 773–785.
550 Sandermann, J.H., 1996. Ozone and plant health. Annu. Rev. Phytopathol. 34, 347–366.
551 Schupp, R., Rennenberg, H., 1988. Diurnal changes in the glutathione content of spruce needles
552 (*Picea abies* L.). Plant Sci. 57, 113–117.
553 Simpson, G.L., Ortwerth, B.J., 2000. The non-oxidative degradation of ascorbic acid at physiological
554 conditions. Biochim. Biophys. Acta BBA-Mol. Basis Dis. 1501, 12–24.
555 Smith, G., Neyra, C., Brennan, E., 1990. The relationship between foliar injury, nitrogen metabolism,
556 and growth parameters in ozonated soybeans. Environ. Pollut. 63, 79–93.
557 Smoydzin, L., Fnais, M., Lelieveld, J., 2012. Ozone pollution over the Arabian Gulf--role of
558 meteorological conditions. Atmospheric Chem. Phys. Discuss. 12, 6331- – 6361.
559 Soobrattee, M.A., Neergheen, V.S., Luximon-Ramma, A., Aruoma, O.I., Bahorun, T., 2005.
560 Phenolics as potential antioxidant therapeutic agents: mechanism and actions. Mutat. Res.
561 Mol. Mech. Mutagen. 579, 200–213.
562 Spence, R.D., Rykiel, E.J., Sharpe, P.J., 1990. Ozone alters carbon allocation in loblolly pine:
563 assessment with carbon-11 labeling. Environ. Pollut. 64, 93–106.

564 Strohm, M., Eiblmeier, M., Langebartels, C., Jouanin, L., Polle, A., Sandermann, H., Rennenberg,
565 H., 1999. Responses of transgenic poplar (*Populus tremula* × *P. alba*) overexpressing
566 glutathione synthetase or glutathione reductase to acute ozone stress: visible injury and leaf
567 gas exchange. J. Exp. Bot. 50, 365–374.
568 Vainonen, J.P., Kangasjärvi, J., 2015. Plant signalling in acute ozone exposure. Plant Cell Environ.
569 38, 240–252.
570 Vanlauwe, B., Nwoke, O.C., Sanginga, N., Merckx, R., 1996. Impact of residue quality on the C and
571 N mineralization of leaf and root residues of three agroforestry species. Plant Soil 183, 221–
572 231.
573 Vanzo, E., Jud, W., Li, Z., Albert, A., Domagalska, M.A., Ghirardo, A., Niederbacher, B., Frenzel,
574 J., Beemster, G.T., Asard, H., 2015. Facing the future - Effects of short-term climate extremes
575 on isoprene-emitting and non-emitting poplar. Plant Physiol. 169, 560-575.
576 Velikova, V., Yordanov, I., Edreva, A., 2000. Oxidative stress and some antioxidant systems in acid
577 rain-treated bean plants: protective role of exogenous polyamines. Plant Sci. 151, 59–66.
578 White, P., Broadley, M.R., Thompson, J.A., McNicol, J.W., Crawley, M.J., Poulton, P.R., Johnston,
579 A.E., 2012. Testing the distinctness of shoot ionomes of angiosperm families using the
580 Rothamsted Park Grass Continuous Hay Experiment. New Phytol. 196, 101–109.
581 Wittig, V.E., Ainsworth, E.A., Long, S.P., 2007. To what extent do current and projected increases
582 in surface ozone affect photosynthesis and stomatal conductance of trees? A meta-analytic
583 review of the last 3 decades of experiments. Plant Cell Environ. 30, 1150–1162.
584 Witzell, J., Martín, J.A., 2008. Phenolic metabolites in the resistance of northern forest trees to
585 pathogens—past experiences and future prospects. Can. J. For. Res. 38, 2711–2727.

586 Xu, B.J., Chang, S.K.C., 2007. A comparative study on phenolic profiles and antioxidant activities
587 of legumes as affected by extraction solvents. J. Food Sci. 72, S159–S166.
588 Yaish, M.W., 2015. Proline accumulation is a general response to abiotic stress in the date palm tree
589 (*Phoenix dactylifera* L.). Genet. Mol. Res. 14, 9943–9950.
590 Zheng, Y., Lyons, T., Barnes, J., 2000. Effects of ozone on the production and utilization of
591 assimilates in *Plantago major*. Environ. Exp. Bot. 43, 171–180.
592 Zhong, D., Du, H., Wang, Z., Huang, B., 2011. Genotypic variation in fatty acid composition and
593 unsaturation levels in bermudagrass associated with leaf dehydration tolerance. J. Am. Soc.
594 Hortic. Sci. 136, 35–40.
595
596

Figures

Fig. 1 Scheme of the experimental design. The acclimation started on 8th June until 27th July, when the ozone exposure was conducted from 10:00 to 18:00. Gas exchange was measured at 1 h, 4 h and 7 h after ozone exposure respectively, in 4 biological replicates for both control and ozone fumigated plants. Leaf samples were harvested after 1 h, 2 h, 4 h and both leaf and root samples were harvested after 8 h ozone fumigation in 6 biological replicates for both control and ozone fumigated plants for each time point.

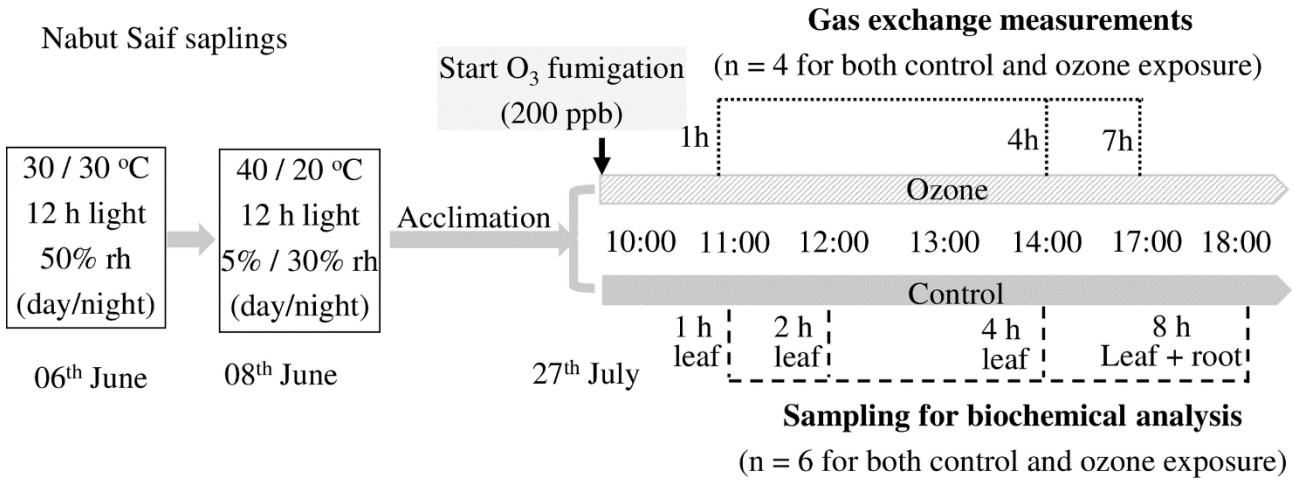

613 Fig. 2 Total sugar (A), soluble protein (B), phenolic compounds (C) and lignin (D) contents of
614 control (grey) and ozone fumigated (dark) plants of date palm. Asterisk indicates significant effect
615 of ozone treatment after 8 h fumigation. Significant differences ($P < 0.05$) between leaves and roots
616 after 8 h ozone treatment were indicated by different letters, upper and lower case letters are for
617 control and ozone fumigated plants respectively. Data shown are means + standard error (n = 6).

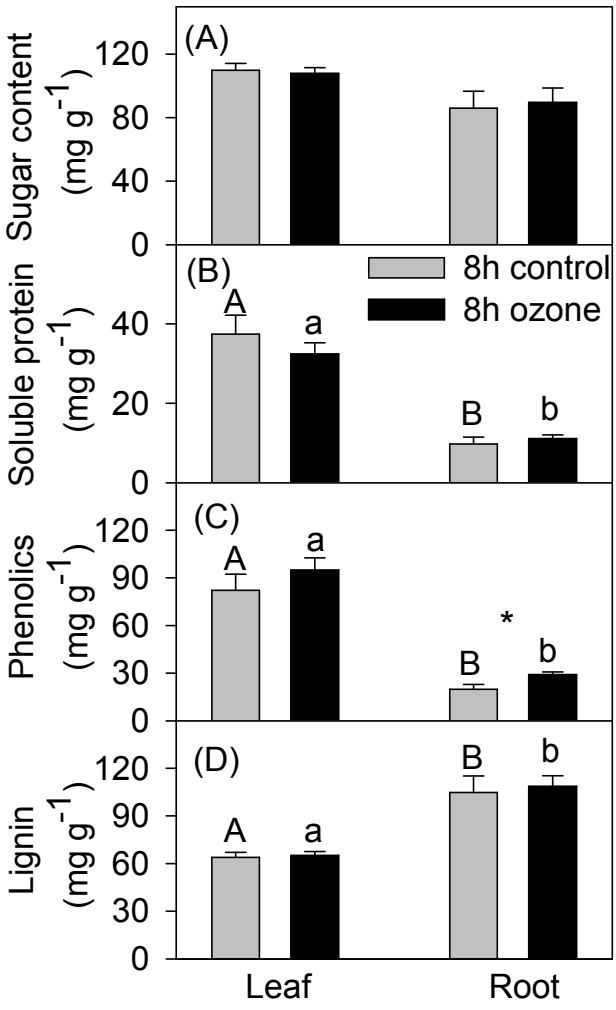

618

Fig. 3 Fold change of metabolites in leaves and roots of date palm after 8 h ozone fumigation. Color scales were generated according to $\log_2$ transferred ratios between the means of ozone treatment and control (n = 6). Red color indicates decreased abundance in ozone exposed plants compared to controls, and blue indicates increased abundance upon ozone fumigation. Significant differences between ozone treatments and controls were indicated by asterisk (*, ** and *** indicate $P < 0.05$, 0.01 and 0.001 respectively). A 'na' means data was not available in both control and treatment plants due to below the detect limitations, '+' means the metabolites only abundant in ozone fumigated plants, and '–' means only abundant in control plants. P: phosphate compounds; IPTG: isopropyl β-D-1-thiogalactopyranoside; NMH-proline: N-methyl trans-4-hydroxy-L-proline (2S,4R)-4-hydroxy-1-methyl pyrrolidine-2-carboxylic acid; DHA: dehydroascorbic acid; 1-P-3-H-5-carboxylate: 1-pyrroline-3-hydroxy-5-carboxylate. Golm Metabolome Database code (MPIMP ID) of each compound was given in Table S3.

631

Groups	Metabolites	+ O_3 / - O_3 Leaf	+ O_3 / - O_3 Root	Leaf / Root - O_3	Leaf / Root + O_3
Sugars	Fructose				
	Glucose			*	
	Lyxose			*	
	Galactose				
	D-cellobiose		na	+	+
	Sucrose				**
	D- α, α'-trehalose				*
	Sophorose			***	**
	Gentiobiose			**	**
	Raffinose			*	
	6-Kestose			***	**
P	Glycerol-3-P			**	
	Mannose-6-P			**	*
Organic acids	Citric acid			*	
	Fumaric acid	*			
	Malic acid				**
	Ribonic acid	*	-		***
	Shikimic acid				
	DHA dimer			***	***
	Isoascorbic acid				*
	Lyxonic acid			***	***
	Hdroxy-hexanedioic acid			***	***
	Succinic acid			*	
Sugar acids	Galactonic acid				
	Glyceric acid			***	***
	Gluconic acid				
	Saccharic acid			***	***
	Threonic acid			***	*
Phenolics	Trans-4-caffeoylquinic acid			**	*
	Catechin			**	***
	4-Hydroxy-benzoic acid	*	**	***	***
	Benzoic acid	na	-	-	na
	Taxifolin	***		***	*
	Guaiacylglycerol			***	**
	Trans-sinapyl alcohol	**			*
	Cis-sinapic acid	**			***
	Lumichrome	na		***	
	Piceatannol				

Groups	Metabolites	+ O_3 / - O_3 Leaf	+ O_3 / - O_3 Root	Leaf / Root - O_3	Leaf / Root + O_3
Nitrogen compounds	Glutamic acid				
	Proline	*		**	**
	NMH-proline				
	Arginine				
	γ-Aminobutyric acid				
	Asparagine				**
	Aspartic acid			*	***
	Threonine				**
	Lysine			*	*
	Alanine	na			
	Valine			**	**
	Leucine			**	**
	Isoleucine			**	*
	Serine				**
	Glycine			*	**
	Phenylalanine				
	Tryptophan				*
	Uracil		*	**	**
	Pyroglutamic acid				*
	Ethanolamine			**	
	Carbodiimide				
	1-P-3-H-5-carboxylate			*	*
Sugar alcohols	Galactinol			***	**
	Arabitol			**	
	Threitol		na	+	+
	Myo-inositol				***
Fatty acids and fatty alcohols	Palmitic acid (C16:0)	+		-	*
	Oleic acid (C18:1)			*	*
	Stearic acid (C18:0)	+		-	
	Stearyl alcohol			***	**
	Heptadecan-1-ol			*	
Others	Phosphoric acid				
	Pipecolinic acid				
	Gluconic acid-1,5-lactone				
	IPTG			***	***
	Gluconic acid-1,4-lactone			**	***
	Glycerolaldopyranosid			***	***
	Threonic acid-1,4-lactone	*		*	**

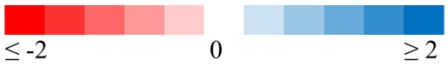

632

633 Fig. 4 Thiols and ascorbate contents of control (grey) and ozone fumigated (dark) date palm.
634 Asterisk indicates significant difference between ozone treatment and control plants (*, $P < 0.05$
635 and **, $P < 0.01$). Significant differences between leaves and roots after 8 h ozone exposure were
636 indicated by different letters, upper and lower case letters are for control and ozone fumigated
637 plants respectively. Data shown are means + standard error (n = 6).

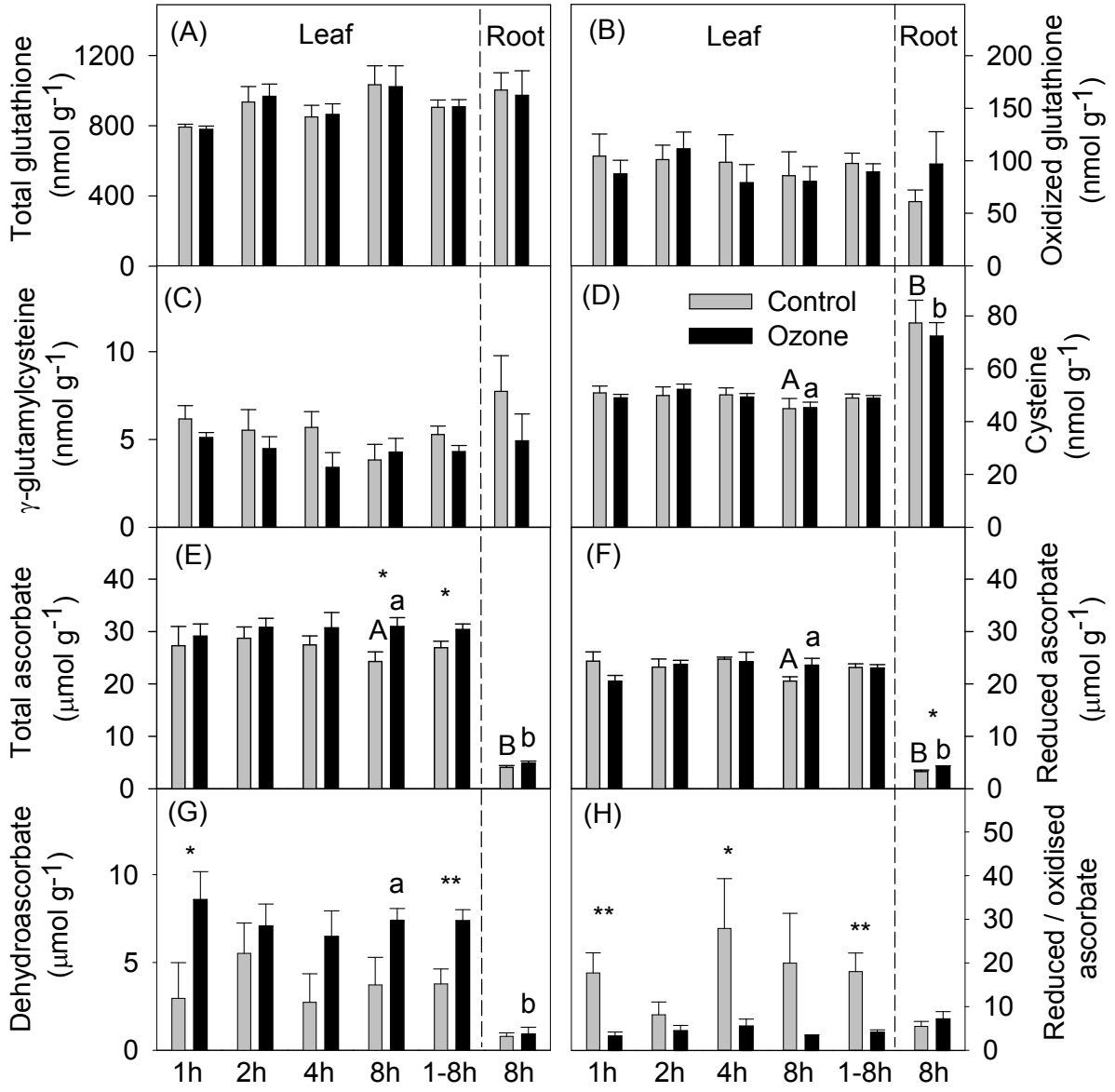

638

639

Fig. 5 Glutathione reductase (GR) (A) and dehydroascorbate reductase (DHAR) (B) activities of control (grey) and ozone fumigated (dark) date palm. Asterisk indicates significant difference between ozone treatment and control plants (*, $P < 0.05$). Significant differences between leaves and roots after 8 h ozone treatment were indicated by different letters, upper and lower case letters are for control and ozone fumigated plants respectively. Data shown are means + standard error (n = 6).

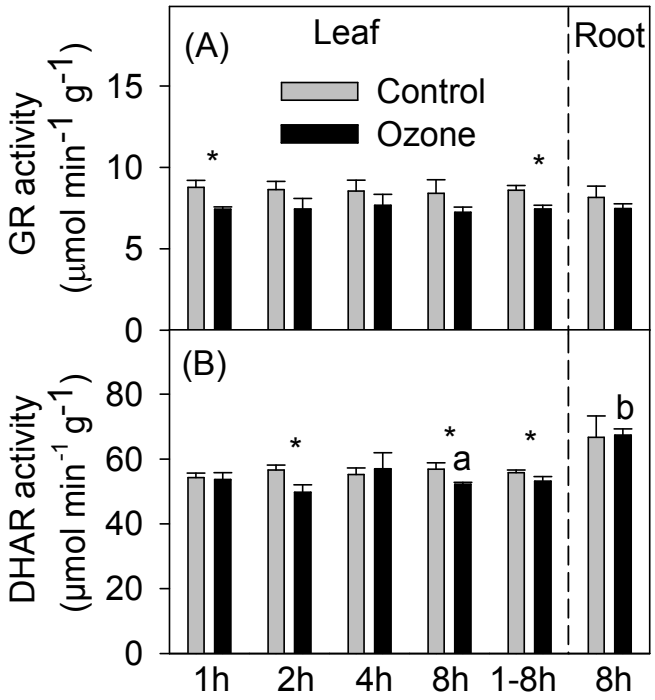

Supplementary Material

S1. Analytical methods

1. Determination of anti-oxidants and hydrogen peroxide

For the determination of the thiol anti-oxidant glutathione (GSH) and its metabolic precursors cysteine and gamma-glutamylcysteine 40 mg frozen leaf or root powder was extracted in 1 ml 0.1 mol HCl containing 100 mg pre-washed polyvinylpolypyrrolidone (PVPP, P6755, Sigma-Aldrich Chemie GmbH, Steinheim, Germany). An aliquot of 50 µl supernatant was mixed with 25 µl 500 mmol 2-cyclochexylamino-ethanosulphonic acid (CHES) buffer (pH 9.3) and 10 µl 15 mmol dithiothereitol (DTT). Determination of oxidized glutathione (GSSG) was based on the irreversible alkylation of the free thiol groups of the GSH present with N-ethylmaleimide (NEM) and the subsequent reduction of GSSG with DTT). For this propose, 10 µL of 5 mmol NEM were added to a second aliquot of 50 µL supernatant of leaf or root extract with 25 µL CHES buffer, but without DTT, and incubated at room temperature for 10 min before adding 10 µl 15 mmol DTT. The reduction of all samples was terminated after 60 min incubation at room temperature by addition of 10 µl 30 mmol monobromobiname for derivatisation. The monobromobine derivatives were stabilized with 55 µl (45 µL for the GSSG batch) 10% (v/v) acetic acid after 15 min derivatisation in the dark. Finally, 100 µl of the reaction solution were transferred into glass vials. Thiol derivatives were separated on an ACQUITY UPLC® HSS (Waters GmbH, Eschborn, Germany), with a C 18 column (2.1 × 50 mm; 1.18 µm) applying a solution of potassium acetate (100 mmol) in methanol (100%) for elution. Concentrations of thiols were quantified with a standard solution mixture consisting of GSH, cysteine and gamma-glutamylcysteine subjected to the same reduction and derivatisation procedure.

Total and reduced ascorbate was determined using the colorimetric method previously described by Arab et al. (2016). Aliquots of 35 mg frozen homogenized leaf and root material were extracted in 500 µL 5% meta-H_3PO_4 solution. After 30 min centrifugation at 4 °C 12000 rpm, aliquots of 100 µL of the supernatant were mixed with 20 µL 1.5 M triethanolamine and 100 µL sodium phosphate buffer (150 mM, pH 7.4). Total ascorbate contents were measured after reduction by adding 50 µL 10 mM DTT and incubation at room temperature for 15 min. The excess DTT was removed by adding 50 µL NEM (0.5%). An aliquot of 100 µL double-distilled H_2O of was added to sample used for the determination of reduced ascorbate instead of DTT and NEM. To all samples 200 µL trichloroacetic acid (TCA, 10%), 200 µL orthophosphoric acid (44%), 200 µL 2,2′-dipyridil (4% in ethanol) and 100 µL $FeCl_3$ (3%) were added and mixed carefully. The absorption of the reaction mixtures was determined with a UV-DU650 spectrophotometer (Beckman Coulter Inc., Fullerton, CA, USA) at 525 nm after incubation at 37 °C in a water bath for 60 min. Concentrations of total and reduced ascorbate were calculated from to a standard curve using L-ascorbic acid (Sigma–Aldrich, Steinheim, Germany) subjected to the same procedure as samples.

H_2O_2 content of leaf and root samples was determined as described by Velikova et al. (2000). Frozen tissue samples of 50 mg were extracted in 0.1% (w/v) trichloroacetic acid (TCA). The homogenate was centrifuged at 15,000 g for 15 min. Aliquots of 300 µL supernatant were combined with 300 µL of 10 mM potassium phosphate buffer (pH 7.0) and 600 µL of 1 M KI. The absorbance of the reaction solutions was measured at 390 nm after 20 min incubation in dark. The content of H_2O_2 was quantified with a standard calibration curve of different concentrations (0 - 200 µM) of H_2O_2.

2. Determination of in vitro activities of glutathione reductase (GR) and dehydroascorbate reductase (DHAR)

47 For the determination of *in vitro* GR (EC-number 1.6.4.2) and DHAR (EC-number 1.8.5.1)
48 activities of leaf and root material aliquots of 100 mg frozen plant material were extracted with 1.5
49 ml ice cold extraction buffer, containing 100 mmol potassium phosphate (pH 7.8), 80 mg PVPP and
50 1% Triton X-100 (v/v). After 10 min incubation on ice, the protein fractions in 500 µL supernatants
51 of the extracts were separated via passing through a Sephadex G-25 column (NAP-5 column, GE
52 Healthcare Life Science, Freiburg, Germany). The columns were washed with 1 ml 100 mmol
53 potassium phosphate buffer (pH 7.8) and eluents were collected for analysis of enzyme activity. GR
54 activity was determined by monitoring glutathione dependent oxidation of 1.25 mmol NADPH at 340
55 nm, DHAR activity was analyzed by following the increase in absorbance at 265 nm, resulting from
56 GSH-dependent production of ascorbate as previously described (Polle et al., 1990). Enzyme
57 measurements were conducted at 40°C, *i.e.* the daytime temperature of plant exposure.
58
59 *3. Hydrogen peroxide analysis*
60 For hydrogen peroxide (H_2O_2) analyses, 50 mg frozen leaf and root samples were extracted in
61 0.1% TCA (w/v). The homogenate was centrifuged at 15,000 *g* for 15 min. Aliquots of 300 µL
62 supernatant were combined with 300 µL 10 mmol potassium phosphate buffer (pH 7.0) and 600 µL
63 1 mol KI. The absorbance of the reaction solutions was measured at 390 nm after 20 min incubation
64 in dark. The content of H_2O_2 was quantified with a standard calibration curve of different H_2O_2
65 concentrations (0 - 200 µmol) (Merck KGaA, Darmstadt, Germany).
66
67
68 *4. Determination of soluble protein, lignin contents and phenolic compounds*

For the determination of total soluble protein 50 mg frozen tissue were extracted in 1.5 ml 50 mmol Tris-HCl containing 1 mmol EDTA, 15% glycerol (v/v), 1 mmol phenylmethylsulfonyl fluoride (PMSF), 5 mmol DTT, 0.1% Triton X-100 and 150 mg acid washed PVPP. The same volume of 10% (w/v) TCA was added and, after 10 min incubation at 4°C, samples were centrifuged at 14,000 g for 15 min. The pellets were dissolved in 1 mol KOH. Soluble protein contents were calculated from the absorbance of the mixture of 5 µL extract with 200 µL Bradford reagent (Amresco Inc., Solon, OH, USA) measured at 595 nm. Bovine serum albumin (Sigma-Aldrich Chemie) was used as reference for quantification.

For lignin analyses, 100 mg dry samples were washed by successive stirring (30 min) and centrifugation (5,000 *g*, 15 min) as follows: 2 times in 10 ml 100 mmol potassium phosphate buffer (pH 7.8, with 1 % Triton X-100, v/v), 4 times in 10 ml 100 % methanol, 2 times in 10 ml 1 mol NaCl and 2 times in 10 ml miliQ water. The pellets were dried in an oven (60°C, 24 h) and the dry matter obtained was defined as protein-free cell wall fraction. For quantification of lignin by the acetyl bromide method, 20 mg of protein-free cell wall sample was weighted into a screw-cap centrifuge tube containing 0.5 ml 25% acetyl bromide (v/v, in glacial acetic acid). The mixture was incubated at 70°C with shanking at 1,200 *g* (Thermo mixer, Eppendorf AG, Hamburg, Germany). After 30 min digestion, the samples were cooled in an ice bath and mixed with 0.9 ml 2 mol NaOH, 0.1 ml 5 mol hydroxylamine-HCl, and 5 ml glacial acetic acid for complete solubilization of the lignin extract. After centrifugation (5,000 *g*, 15 min), the absorbance of the supernatant was measured at 280 nm. A standard curve was generated with alkali lignin (Sigma-Aldrich Chemie) subjected to the same procedure. The results were expressed as mg lignin g^{-1} dw.

Total phenolic compounds in plant samples were extracted with 50% acetone and quantified by the Folin-Denis method using gallic acid as standard. Approximately 50 mg frozen leaf or root

92 powder was extracted three times with 1 ml 50% acetone (4 °C, 15 min incubation with shaking).
93 Aliquots of 40 µL of the combined extracts were mixed with 1560 µL miliQ water and 100 µL Folin-
94 Denis reagent (Sigma-Aldrich, Steinheim, Germany). After 8 min, 300 µL 20% Na_2CO_3 (dissolved
95 in milliQ water, w/v) was add to each tube and mixed thoroughly. The absorption at 765 nm was
96 determined after 20 min with a UV-DU650 spectrophotometer (Beckman Coulter Inc., Fullerton, CA,
97 USA). The total phenolic content was expressed as gallic acid equivalents (mg g^{-1} dw of sample)
98 determined by a calibration curve with gallic acid.
99
100 *5. Determination of ions and elements*
101 For the determination of anion contents, aliquots of 50 mg of leaf or root powder and 100 mg
102 PVPP were mixed with 1 ml double-distilled H_2O for 1 h at 4°C under continuous shaking. After
103 boiling for 10 min to precipitate proteins, the extracts were centrifuged for 10 min at 14,000 g.
104 Aliquots of 50 µL of the supernatants were injected into an ion chromatography system (DX 120,
105 Dionex, Idstein, Germany). Separation of anions was achieved by an ion exchange column (AS12A,
106 4 mm, Dionex) with 2.0 mmol Na_2CO_3 and 0.75 mmol $NaHCO_3$ as mobile phase. Detection and
107 quantification was performed with a pulsed amperometric detector (Electrochemical detector ED 40
108 Dionex). Sodium salts of nitrate, phosphate, and sulphate were used as standards for quantification.
109 For determination of tissue potassium (K), calcium (Ca), magnesium (Mg), phosphorus (P),
110 sulphur (S), sodium (Na), chloride (Cl), iron (Fe), manganese (Mn), zinc (Zn), copper (Cu) and nickel
111 (Ni) concentrations, freeze dried tissue samples were placed in an oven at 70 °C overnight prior to
112 analysis. Ca. 50 mg dried subsamples were weighted and digested in closed vessels using a
113 microwave digester (MARS Xpress, CEM Microwave Technology, Buckingham, UK). Samples were
114 first digested with 10 ml concentrated nitric acid (HNO_3), before 3 ml of 30% H_2O_2 was added to

each vessel to complete digestion. Digested samples were diluted with milliQ water before element analyses. Total K, Ca, Mg, P, S, Na, Cl, Fe, Mn, Zn, Cu and Ni concentrations were determined on digested material by ICP-MS (ELAN DRCe, PerkinElmer, Waltham, MA, USA). Blank digestions were performed to determine background concentrations of elements and a tomato leaf standard (Reference 1573a; National Institute of Standards and Technology, NIST, Gaithersburg, MD, USA) was used as an analytical control.

6. Extraction and determination of water soluble metabolites

Approximately 50 mg of frozen powder was weighted into a pre-cooled 2 ml reaction tube, then 600 µl cold 100% methanol and 60 µl ribitol (0.2 mg ml^{-1}) were added, the latter as internal standard. Tubes were vortexed briefly, heated to 70°C and shaken at 1,200 *g* for 10 min. Samples were centrifuged at 14,000 *g* for 5 min; then 500 µl supernatant was combined with 500 µl milliQ water and 500 µl cold chloroform. The mixtures were intensively shaken and centrifuged at 14,000 *g* for another 5 min. An aliquot of 100 µl of the supernatant from the methanol phase was freeze-dried for 48 h. For derivatization, 20 µl of a 20 mg ml^{-1} solution of methoxyamine hydrochloride in anhydrous pyridine (Sigma-Aldrich Chemie) was added to the dried extracts and samples were incubated at 30 °C for 90 min with shaking at 1,400 *g*. Thereafter, 40 µl N-methyl-N-(trimethylsilyl)-trifluoroacetamide (MSTFA, Sigma-Aldrich Chemie) were added and samples were incubated at 37 °C for 30 min with shaking at 1,200 *g*. Then, 50 µl solution was transferred into glass vials with inserts and sealed for GC-MS analysis. A mixture of n-alkane (C8-C20, saturated alkane mixture, Sigma-Aldrich Chemie) was measured together with samples for retention index calibration.

A GC-MS system (Agilent GC 6890N coupled to a 5975C quadrupole MS detector; Agilent Technologies, Palo Alto, CA, USA) equipped with an autosampler (MultiPurpose Sampler MPS2;

Gerstel, Mülheim, Germany) was employed for analysis of the samples. Aliquots of 1 µl derivatized sample were injected in splitless mode into the system and separated on a capillary column (HP-5 ms ultra inert, 0.25 mm ID, 0.25 µm film thickness, 30 m length; Merck). The GC-MS system was controlled by the Agilent Masshunter software (Agilent Technologies). Peak detection and alignment was performed with the Quantitative Analysis Module of the Masshunter software. A relative quantification of metabolites was done by calculating the peak areas of the chromatograms after normalization using the peak area of the internal standard, ribitol, and the dry weight of samples. Artefact peaks and common contaminants were identified by analysis of 'blank' samples prepared in the same manner as biological samples. Signals corresponding to these artefacts were omitted from biological interpretation.

Fig. S1. Gas exchange parameters of control (grey) and ozone fumigated (dark) Date palm. iWUE, the calculated instantaneous intrinsic water use efficiency; Ci/Ca, CO_2 concentration ratio between intracellular and ambient. Data shown are means + standard error (n = 4). Statistical significant differences between ozone exposed plants and controls were not observed.

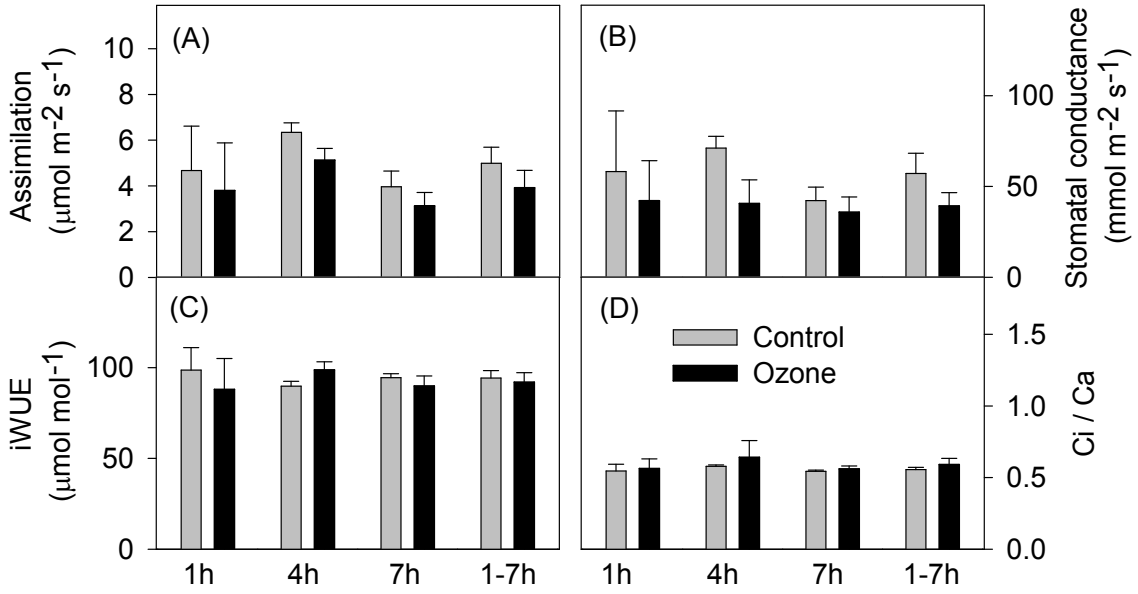

Table S1 Hydration, total C, N, $\delta^{13}C$, $\delta^{15}N$ and hydrogen peroxide contents of control and ozone fumigated date palm seedling. Data shown are means ± standard error (n = 6) of per gram dry weight basis. No significant ($P < 0.05$) effect of ozone was found on these parameters. Significant differences between leaves and roots are indicated by different letters, upper and lower case letters are for control and ozone fumigated plants, respectively.

		Leaf					Root
Parameters	Treatment	1h	2h	4h	8h	1-8h	8h
Hydration	Control	1.88±0.03	1.95±0.05	1.89±0.04	1.85±0.01 ^{A}	1.89±0.02	3.25±0.35 ^{B}
(g H_2O g^{-1})	Ozone	1.92±0.06	1.91±0.06	1.89±0.05	1.84±0.03 ^{a}	1.89±0.02	3.02±0.29 ^{b}
Total C (mg g^{-1})	Control	475.69±4.82	468.59±4.74	474.13±4.90	483.21±11.65	475.46±3.60	463.11±5.92
	Ozone	480.21±6.32	473.27±2.23	475.41±5.96	475.31±3.99	476.05±2.28	463.85±1.77
Total N (mg g^{-1})	Control	14.88±0.35	15.97±1.33	15.44±0.81	16.43±1.05 ^{A}	15.69±0.47	9.51±1.85 ^{B}
	Ozone	14.66±0.17	15.31±0.58	13.90±0.37	14.87±0.56 ^{a}	14.68±0.23	6.58±0.89 ^{b}
C / N ratio	Control	32.08±0.98	30.14±1.98	31.00±1.38	29.89±1.57 ^{A}	30.77±0.74	56.61±9.06 ^{B}
	Ozone	32.78±0.61	31.14±1.25	34.30±0.97	32.23±1.43 ^{a}	32.61±0.56	77.40±10.42 ^{b}
□^{13}C (‰)	Control	-28.51±0.35	-27.63±0.68	-28.06±0.85	-27.47±0.32 ^{A}	-27.91±0.28	-26.03±0.24 ^{B}
	Ozone	-27.60±0.48	-27.98±0.40	-27.90±0.94	-27.86±0.42 ^{a}	-27.83±0.27	-25.68±0.55 ^{b}
□^{15}N (‰)	Control	1.43±0.40	2.05±0.30	1.77±0.23	1.26±0.49	1.62±0.19	1.60±0.55
	Ozone	2.27±0.26	2.06±0.59	2.11±0.25	2.31±0.15	2.19±0.16	2.17±0.33
H_2O_2 (µmol g^{-1})	Control	3.80±0.24	4.23±0.48	3.63±0.30	4.11±0.23 ^{A}	3.96±0.16	0.98±0.12 ^{B}
	Ozone	3.77±0.09	3.78±0.21	4.05±0.37	4.12±0.33 ^{a}	3.93±0.13	1.10±0.21 ^{b}

Table S2 Anions and ions contents (in per gram dry weight) of control and ozone fumigated date palm. Bold indicates significant ozone effects between ozone treatment and control plants within the same time ($P < 0.05$). Significant differences between leaves and roots after 8 h ozone treatment were indicated by different letters, upper and lower case letters are for control and ozone fumigated plants respectively. Data shown are means ± standard error (n = 6).

		Leaf					Root
Parameters	Treatment	1h	2h	4h	8h	1-8h	8h
NO_3^- (μmol g^{-1})	Control	**2.09±0.39**	**2.18±0.32**	2.11±0.39	**1.72±0.29** ^{A}	**2.03±0.17**	**112.79±28.27** ^{B}
	Ozone	**0.64±0.37**	**0.63±0.42**	1.08±0.39	**0.59±0.26** ^{a}	**0.74±0.17**	**40.40±5.53** ^{b}
PO_4^{3-} (μmol g^{-1})	Control	298.05±44.20	**493.01±129.66**	264.26±30.62	348.42±54.03 ^{A}	**354.7±40.08**	162.32±12.92 ^{B}
	Ozone	188.02±37.15	**214.21±42.96**	243.59±39.58	223.49±33.03 ^{a}	**217.33±18.36**	111.86±32.01 ^{b}
SO_4^{2-} (μmol g^{-1})	Control	**183.13±19.82**	**204.18±7.69**	151.24±32.14	123.85±14.93	**166.23±11.29**	157.26±13.82
	Ozone	**96.10±13.73**	**138.98±16.23**	108.61±21.68	119.58±13.85	**115.82±8.45**	121.9±29.36
Na (mg g^{-1})	Control	0.14±0.01	0.13±0.01	0.11±0.01	0.12±0.01 ^{A}	0.12±0.01	0.32±0.03 ^{B}
	Ozone	0.13±0.02	0.14±0.02	0.13±0.01	0.11±0.01 ^{a}	0.13±0.01	0.27±0.04 ^{b}
Mg (mg g^{-1})	Control	2.92±0.12	2.83±0.15	2.81±0.12	2.76±0.06	2.83±0.06	2.53±0.23
	Ozone	2.75±0.16	2.93±0.12	2.68±0.21	2.76±0.07	2.78±0.07	2.44±0.25
P (mg g^{-1})	Control	2.65±0.27	3.76±0.80	2.70±0.18	3.34±0.44 ^{A}	3.13±0.25	2.13±0.19 ^{B}
	Ozone	2.59±0.42	2.88±0.46	3.08±0.37	2.70±0.29 ^{a}	2.81±0.19	1.95±0.16 ^{b}
S (mg g^{-1})	Control	2.70±0.12	2.73±0.15	2.57±0.19	2.44±0.08	2.61±0.07	3.08±0.29
	Ozone	2.32±0.14	2.70±0.16	2.32±0.22	2.48±0.13	2.45±0.08	2.40±0.17
Cl (mg g^{-1})	Control	**10.79±1.48**	8.06±1.59	9.83±1.53	8.78±1.19	**9.34±0.71**	**6.73±0.86**
	Ozone	**6.32±0.81**	5.92±1.11	6.92±1.04	7.78±1.95	**6.74±0.62**	**9.42±0.71**
K (mg g^{-1})	Control	18.26±0.86	20.53±1.97	19.58±0.19	20.13±1.18	19.63±0.61	18.25±1.51
	Ozone	18.10±0.45	18.97±0.80	18.94±0.69	18.57±0.85	18.65±0.34	17.33±0.94
Ca (mg g^{-1})	Control	9.24±0.61	9.66±0.39	8.59±0.28	9.56±0.42 ^{A}	9.29±0.22	3.78±0.44 ^{B}
	Ozone	9.25±0.92	10.08±0.68	9.63±0.82	9.57±0.76 ^{a}	9.63±0.38	3.42±0.31 ^{b}
Mn (mg g^{-1})	Control	0.14±0.04	0.18±0.02	0.19±0.01	0.19±0.03 ^{A}	**0.17±0.01**	0.03±0.01 ^{B}
	Ozone	0.12±0.02	0.14±0.02	0.14±0.02	0.16±0.02 ^{a}	**0.14±0.01**	0.03±0.01 ^{b}
Zn (μg g^{-1})	Control	16.74±1.23	18.96±1.61	16.36±1.13	18.78±1.56	17.77±0.70	15.79±2.32
	Ozone	17.90±1.02	19.81±1.55	17.36±1.42	16.04±1.25	17.78±0.68	20.42±4.41
Fe (μg g^{-1})	Control	45.02±3.00	46.10±3.46	39.50±2.58	41.93±1.43	43.29±1.38	43.18±5.83
	Ozone	42.05±4.00	44.65±2.22	42.39±3.46	43.66±3.34	43.19±1.56	43.96±6.61
Cu (ng g^{-1})	Control	1.78±0.15	2.03±0.30	1.73±0.08	2.41±0.28	2.00±0.12	3.12±0.25
	Ozone	1.60±0.29	1.74±0.24	1.83±0.25	2.01±0.25	1.79±0.12	2.98±0.36
Ni (ng g^{-1})	Control	0.45±0.08	0.31±0.03	0.26±0.02	0.35±0.03	0.35±0.03	0.27±0.04
	Ozone	0.29±0.04	0.40±0.04	0.37±0.06	0.51±0.14	0.39±0.04	0.25±0.02

Table S3 Golm Metabolome Database codes (MPIMP ID) of identified metabolites. IPTG: isopropyl β-D-1-thiogalactopyranoside; NMH-proline: N-methyl trans-4-hydroxy-L-proline (2S,4R)-4-hydroxy-1-methyl pyrrolidine-2-carboxylic acid; DHA: dehydroascorbic acid; 1-P-3-H-5-carboxylate: 1-pyrroline-3-hydroxy-5-carboxylate.

Groups	Metabolites	Match factor	MPIMP ID	Groups	Metabolites	Match factor	MPIMP ID
Sugars	Fructose	84	A187002	Nitrogen compounds	Glutamic acid	65	A154002
	Glucose	82	A189005		Proline	81	A117006
	Lyxose	81	A165006		NMH-proline	75	R002953
	Galactose	85	A188001		Arginine	70	A176005
	D-cellobiose	75	A278010		γ-Aminobutyric acid	70	A153003
	Sucrose	87	A264001		Asparagine	86	A151002
	D- α, α'-trehalose	86	A274002		Aspartic acid	75	A144003
	Sophorose	81	A275015		Threonine	71	A132001
	Gentiobiose	86	A285003		Lysine	63	A186002
	Raffinose	87	A337002		Alanine	81	A138002
	6-Kestose	71	A341001		Valine	71	A109001
Phosphates	Glycerol-3-P	72	A177002		Leucine	65	A118001
	Mannose-6-P	80	A231001		Isoleucine	71	A119002
Organic acids	Citric acid	79	A182004		Serine	75	A128001
	Fumaric acid	71	A137001		Glycine	61	A114001
	Malic acid	87	A149001		Phenylalanine	60	R002940
	Ribonic acid	69	A177001		Tryptophan	60	A219006
	Shikimic acid	82	A181002		Uracil	63	A136001
	DHA dimer	74	A185002		Pyroglutamic acid	60	A151009
	Isoascorbic acid	67	A196002		Ethanolamine	77	A128002
	Lyxonic acid	79	A178005		Carbodiimide	83	A100005
	Hdroxy-hexanedioic acid	60	A168005		1-P-3-H-5-carboxylate	77	A151025
	Succinic acid	60	A134001	Sugar alcohols	Galactinol	87	A299002
Sugar acids	Galactonic acid	70	A199002		Arabitol	67	A171012
	Glyceric acid	73	A135003		Threitol	76	A149002
	Gluconic acid	76	A200001		Myo-inositol	84	A209002
	Saccharic acid	63	A201001	Fatty acids and fatty alcohols	Palmitic acid (C16:0)	78	A205001
	Threonic acid	65	A156001		Oleic acid (C18:1)	60	A223003
Phenolics	Trans-4-caffeoylquinic acid	66	A317001		Stearic acid (C18:0)	69	A225002
	Catechin	83	A289005		Stearyl alcohol	69	A215001
	4-Hydroxy-benzoic acid	79	A164003		Heptadecan-1-ol	60	A203007
	Benzoic acid	81	A128003	Others	Phosphoric acid	90	A129001
	Taxifolin	68	A296005		Pipecolinic acid	69	R000477
	Guaiacylglycerol	75	R003100		Gluconic acid-1,5-lactone	67	A189008
	Trans-sinapyl alcohol	60	A209005		IPTG	77	M001041
	Cis-sinapic acid	60	A207001		Gluconic acid-1,4-lactone	66	A189013
	Lumichrome	87	R001472		Glycerolaldopyranosid	75	A231002
	Piceatannol	61	A286012		Threonic acid-1,4-lactone	60	A140005